

Experimental Study of the Fermi Surfaces of Niobium and Tantalum

M. H. HALLORAN

University of Southern California, Los Angeles, California 90024

AND

J. H. CONDON, J. E. GRAEBNER, J. E. KUNZLER, AND F. S. L. HSU

Bell Telephone Laboratories, Murray Hill, New Jersey 07974

(Received 26 June 1969)

The Fermi surfaces of niobium and tantalum have been investigated experimentally utilizing the techniques of the de Haas-van Alphen effect at magnetic fields up to 31 kOe and magnetothermal oscillations at magnetic fields up to 110 kOe. Oscillations associated with extremal orbits on two Fermi-surface sheets of each element have been observed. The Fermi surface is found to have qualitatively the same topology in both metals: a set of six closed surfaces substantially distorted from ellipsoidal shape and centered at N in the bcc Brillouin zone; and a multiply connected jungle-gym surface consisting of interconnecting arms along $\langle 100 \rangle$ directions with intersections at Γ and H . The agreement between these data and recent augmented-plane-wave (APW) energy-band calculations is excellent. The minimum cross sections of the $\langle 100 \rangle$ arms of the jungle gym have areas of 0.138 \AA^{-2} in Nb and 0.263 \AA^{-2} in Ta; and the principal cross sections of the distorted ellipsoids are 0.636 , 0.757 , and 0.857 \AA^{-2} in Nb, and 0.434 , 0.580 , and 0.59 \AA^{-2} in Ta. A third surface of holes centered at Γ is predicted by band-structure calculations, but has not been observed unambiguously in the present work. Effective masses have been measured at several orientations, and comparison with the APW calculations yield average mass-enhancement factors of 1.75 for Nb and 1.85 for Ta, in fair agreement with predictions based on phonon enhancement.

I. INTRODUCTION

THIS paper presents the results of a series of experiments using the de Haas-van Alphen (dHvA) effect and magnetothermal oscillations¹ (MTO) to determine the Fermi surfaces of two transition metals, niobium and tantalum. These belong to the vanadium group (VB) of transition metals, have the bcc structure, and are characterized by a large electronic heat capacity and relatively high superconducting transition temperatures. An early indication of the gross features of the Fermi surface was given several years ago in a paper by Mattheiss² primarily concerned with the band structure of tungsten. Recently Deegan and Twose³ reported detailed results of a modified OPW calculation of the band structure of Nb. Mattheiss⁴ has also recently completed detailed APW calculations for both Nb and Ta, including the Fermi-surface topology and band effective masses. Our results will be compared to this latter model, and differences between calculated and measured masses will be compared with estimates⁵ of mass enhancement due to electron-phonon interaction.

In the past, experimental results⁶ in Nb and Ta were limited by sample purity and the availability of magnetic fields which are sufficiently high, homogeneous, and stable. More recently, Fawcett, Reed, and Soden⁷ have made single crystals with resistance ratios

approaching 10 000 and have used them to determine the high-field galvanomagnetic properties. Their results verified that Nb and Ta are uncompensated with a net carrier concentration of one hole per atom and indicated a Fermi surface which includes a set of interconnecting cylinders along the cube axes, as predicted by Mattheiss.^{2,4} Samples from the same crystals were used to obtain the first detailed Fermi-surface results in Nb and Ta^{8,9} and in the present work. Scott, Springford, and Stockton have recently studied the dHvA effect in Nb,¹⁰ and in general their results are in agreement with the present work.

II. EXPERIMENTAL DETAILS

The experimental work was performed in three phases. First,⁸ the dHvA effect of Ta was studied with a torsion balance in magnetic fields up to 31 kOe using an iron core electromagnet. Secondly,⁹ MTO of both elements were studied in a 60-kOe superconducting solenoid using an apparatus which provided for the adiabatic rotation of the sample in the magnetic field that is described elsewhere.¹¹ Finally, further measurements were carried out with the same apparatus in a Nb₃Sn superconducting solenoid which was capable of producing magnetic fields up to 110 kOe. In the last stage of the work, computer calculation of the Fourier

¹ J. E. Kunzler, F. S. L. Hsu, and W. S. Boyle, *Phys. Rev.* **128**, 1084 (1962).

² L. F. Mattheiss, *Phys. Rev.* **139**, A1893 (1965).

³ R. A. Deegan and W. D. Twose, *Phys. Rev.* **164**, 993 (1967).

⁴ L. F. Mattheiss, following paper, *Phys. Rev. B* **1**, 373 (1970).

⁵ W. L. McMillan, *Phys. Rev.* **167**, 331 (1968).

⁶ A. G. Thorsen and T. G. Berlincourt, *Phys. Rev. Letters* **7**, 244 (1961).

⁷ E. Fawcett, W. A. Reed, and R. R. Soden, *Phys. Rev.* **159**, 533 (1967); W. A. Reed and R. R. Soden, *ibid.* **173**, 677 (1968).

⁸ J. H. Condon, *Bull. Am. Phys. Soc.* **11**, 170 (1966).

⁹ M. H. Halloran, F. S. L. Hsu, and J. E. Kunzler, *Bull. Am. Phys. Soc.* **13**, 59 (1968).

¹⁰ G. B. Scott, M. Springford, and J. R. Stockton, *Phys. Letters* **27A**, 655 (1968); also G. B. Scott, M. Springford, and J. R. Stockton, in *Proceedings of the Eleventh International Conference on Low Temperature Physics, St. Andrews, 1968* (University of St. Andrews Printing Department, Edinburgh, 1969), p. 1129.

¹¹ M. H. Halloran and J. E. Kunzler, *Rev. Sci. Instr.* **39**, 1501 (1968).

transform of some of the data provided improved resolution and sensitivity.

The 60-kOe solenoid calibration was provided by the manufacturer as a field-versus-current relationship with quoted accuracy of $\lesssim 0.3\%$. The field was also measured using a cryogenic Hall probe¹² with a constant current source. At a current of 1 mA this probe had an average sensitivity of approximately $0.5 \mu\text{V/G}$ at 1.2 K with a very slight temperature dependence in that range. Higher currents tended to warm the sample as well as the Hall probe, since the Hall probe was mounted in the evacuated sample chamber as near as possible to the sample. Sample temperature changes were detected with carbon resistance thermometers having temperature sensitivities of 10^{-6} – $10^{-6} \Omega/^{\circ}\text{K}$ at $T=1.2 \text{ K}$.

Since the 110-kOe solenoid was energized by a flux pump there was no way of measuring the current through the solenoid. Therefore a copper wire magneto-resistance probe¹³ was used to measure the field. It had been previously calibrated with the nuclear magnetic resonance of ^{157}Cs located at the sample site.¹⁴

Field modulation in both solenoids was provided by auxiliary solenoids made of a few layers of fine superconducting wire which were inserted between the main solenoid and the Dewar containing the experimental apparatus. This permitted direct measurement of $\partial T/\partial H$ with phase-sensitive detection techniques enhancing the sensitivity of the experiments, and all MTO data presented here were obtained in this manner.

The samples were sections $\sim 10 \text{ mm}$ long spark cut from rods of $\sim 3 \text{ mm}$ diam which had resistance ratios $R_{273\text{K}}/R_{4.2\text{K}}$ of ~ 3000 for Nb and $\sim 10\,000$ for Ta.⁷ They were oriented to within $\sim 2^{\circ}$ using standard Laue x-ray techniques.

All experiments were performed at temperatures in the range of 1.1–2.0 K, as determined by the vapor pressure of the helium bath measured with a McLeod gauge.

III. APW MODEL OF FERMI SURFACE

The Fermi surfaces obtained by Mattheiss⁴ for Nb and Ta are qualitatively very similar and therefore only the one for Nb is shown in Fig. 1; Fig. 1(a) shows the closed second-zone hole surface centered at Γ , which is in the form of a distorted sphere and calculated to have a rather large band mass $[(1.4\text{--}2.0) m_0]$. Orbits attributed to this surface will be designated γ_1 orbits. Figure 1(b) shows the open surface of holes in the third zone which is characterized by arms along the $\langle 100 \rangle$ directions intersecting at both Γ and H and referred to as the jungle-gym surface. Orbits around the arms will be designated α orbits and are expected to have relatively small band masses $[(0.7\text{--}0.8) m_0]$, but orbits about the intersections (designated η orbits if centered at H and γ_2 if centered at Γ) should have appreciably

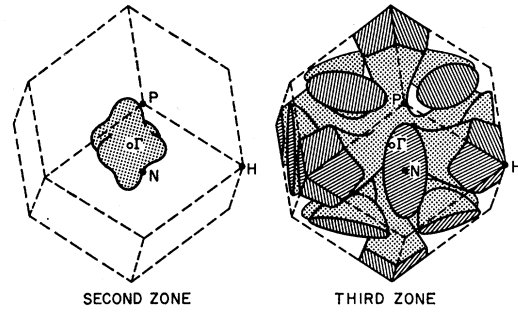


FIG. 1. Calculated Fermi surface of niobium; (a) closed second-zone hole surface centered at Γ , (b) third-zone hole surfaces including the open jungle-gym surface and the set of six distorted ellipsoids which are indexed according to the numbers in the figure.

larger band masses $[(1.2\text{--}1.5) m_0$ for η orbits and $(1.9\text{--}2.2) m_0$ for γ_2 orbits]. The jungle-gym surface and the second-zone surface at Γ are distorted from the shape shown in Fig. 1, thus permitting noncentral η and γ_1 orbits over certain ranges in angle as discussed in Sec. IV. Electron orbits are also possible around the closed path formed by four arms of the jungle gym in and near $\{100\}$ planes. These will be designated as Δ orbits and are expected to have a large band mass $[(1.3\text{--}1.7) m_0]$. Figure 1(b) also shows the closed hole surfaces centered at N in the third zone which have more or less the shape of ellipsoids but with large bulges toward Γ . These surfaces support orbits which will be designated as ν_i orbits, where the subscript i defines the particular ellipsoid following the convention of Mattheiss,⁴ and have masses comparable to or slightly larger than α orbits. (There was some uncertainty in the early calculations² concerning the possibility of the warped ellipsoids joining together at P or joining with the jungle gym along the ΓN line. These possibilities were more probable for Nb, which has larger ellipsoids, although the later galvanomagnetic measurements⁷ and band calculations⁴ indicate that no contact occurs in either material.) A summary of the calculated cross-sectional areas and effective masses for specific symmetry directions is given in Table II of Ref. 4.

In the absence of spin-orbit coupling, there is an accidental degeneracy between the second-zone hole surface and third-zone jungle gym, the former lying within the latter but touching at several points in the $\{100\}$ and $\{110\}$ planes. Although spin orbit coupling removes these degeneracies, the splittings may be small, especially in niobium, thereby permitting magnetic breakdown to occur for certain field directions.

The band calculations are sufficiently precise to place some confidence in the calculated band mass. This enables comparison of observed cyclotron masses with the band masses to determine the mass enhancement factor. This factor due to electron-phonon interactions has been estimated by McMillan⁵ to be 1.82 and 1.65 for Nb and Ta, respectively. McMillan has also suggested that these enhancement factors for

¹² Siemens Hall probe, model SV210T.

¹³ F. S. L. Hsu and J. E. Kunzler, Rev. Sci. Instr. **34**, 297 (1963).

¹⁴ L. W. Rupp, Jr., Rev. Sci. Instr. **37**, 1039 (1966).

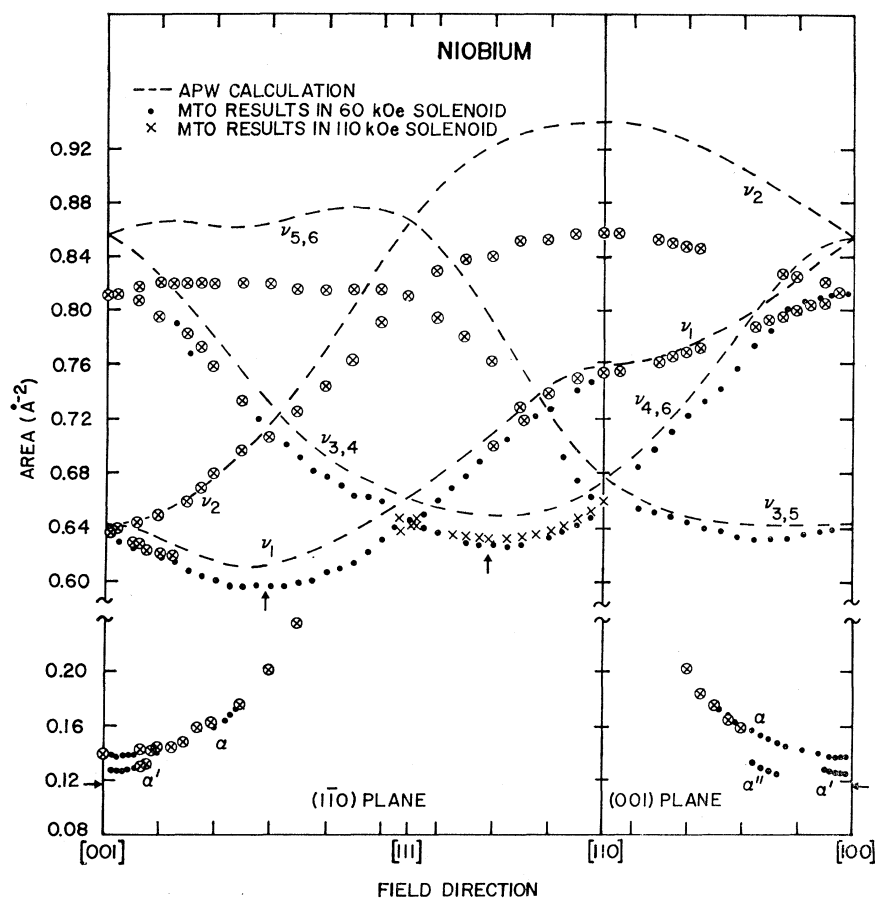


FIG. 2. Extremal Fermi-surface areas in niobium as a function of angle in the (110) and (001) planes for ellipsoids and jungle-gym arms. Vertical arrows indicate positions of relative minima in area as determined from rotation data, and horizontal arrows indicate the calculated minimum area of the jungle-gym arms. Circles around data points indicate computer reduction of the data.

individual orbits may be anisotropic and evidence favoring this possibility in other transition metals has been obtained recently.¹⁵

IV. RESULTS

A. General Features

The dependence on crystallographic orientation of the frequencies observed in the (110) and (001) planes are shown in Figs. 2 and 3 for Nb and Ta, respectively. These include torsion balance dHvA results in Ta as well as the MTO results in both Nb and Ta. Torsion balance dHvA oscillations were observed in Nb also, but with very small amplitude. Additional frequencies that were found near the $\langle 111 \rangle$ directions are shown in Figs. 4 and 5. The predictions of the APW calculation⁴ are also indicated in the figures. In these figures, we have plotted the extremal Fermi-surface areas corresponding to the observed frequencies, rather than the frequencies themselves.

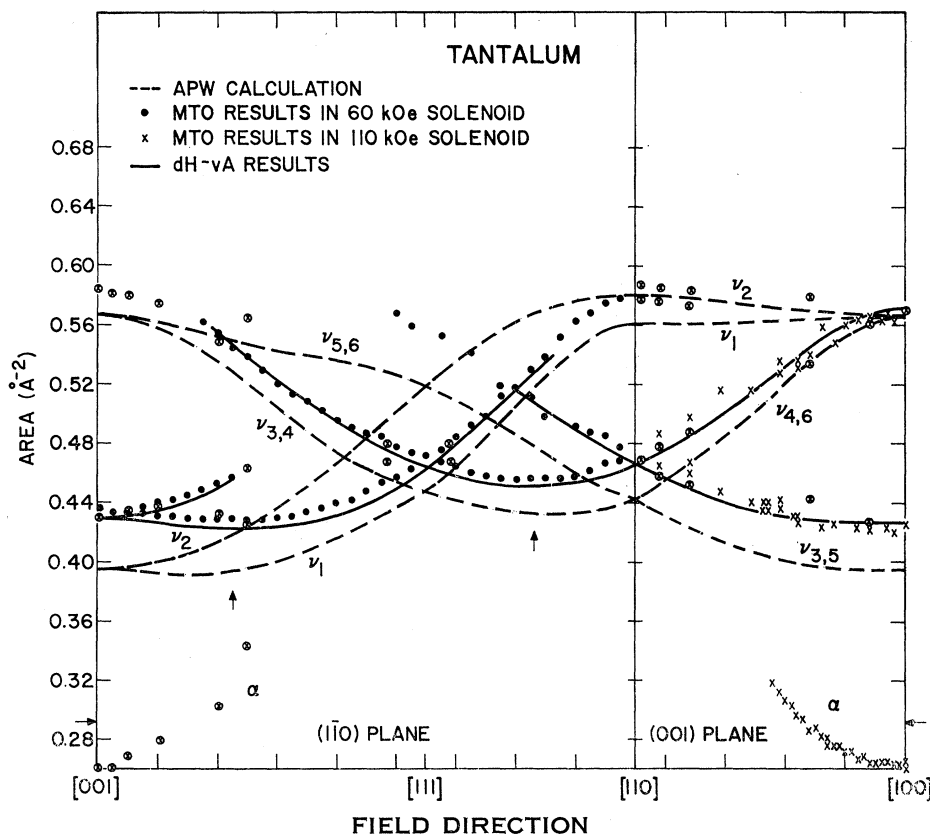
It is clear from Figs. 2-5 that the results in Ta and Nb are qualitatively similar. This similarity makes it possible to discuss the results in both materials at the

same time. The ν_i branches due to the distorted ellipsoids centered at N dominate the data in most regions. Near the $[100]$ axis the α orbits about the jungle-gym arms are observed in both symmetry planes over a range of approximately 25° in Ta and 35° in Nb. In addition there are other frequencies, α' , observed in Nb near the $[100]$ axis of nearly the same frequency as the α oscillations. Another set of frequencies again very nearly equal in frequency to the α orbits is observed in Nb about 15° away from the $[100]$ axis in the (100) plane. These frequencies are designated α'' and have an angular range of approximately 6° . No oscillations analogous to α' or α'' were observed in Ta. Finally, larger frequencies observed with MTO near the $[111]$ axis at fields near 100 kOe in both Nb and Ta are attributed to η orbits about the H intersection of the jungle gym.

It is also clear from Figs. 2-5 that the experimental data and the APW calculation agree well, generally within a few percent. The region of largest percentage deviation between experiment and theory is for the α orbits about the minimum area of the jungle-gym arms in Nb, which is a relatively small area and very sensitive to slight shifts in the Fermi energy. Other deviations indicate that the NTP area of each ellipsoid

¹⁵ J. B. Ketterson and L. R. Windmiller, Phys. Rev. Letters **20**, 321 (1968).

FIG. 3. Extremal Fermi-surface areas in tantalum as a function of angle in $(1\bar{1}0)$ and (001) planes for ellipsoids and jungle-gym arms. Arrows indicate position of relative minima in area as determined from rotation data, and horizontal arrows indicate the calculated minimum area of the jungle-gym arms. Circles around data points indicate computer reduction of the data.



in Nb is $\sim 10\%$ larger than calculated, and the NTH area of each ellipsoid in Ta is $\sim 10\%$ larger than calculated. Some other orbits predicted by the calculation but not observed in the data are all predicted to have larger effective masses and are assumed to be unobservable within the field and temperature range of the present experiments.

The early and quite limited data of Thorsen and Berlincourt⁶ agree well with ours in Ta but poorly in Nb.

The recent dHvA frequency data of Scott, Springfield, and Stockton¹⁰ substantially confirm our data in

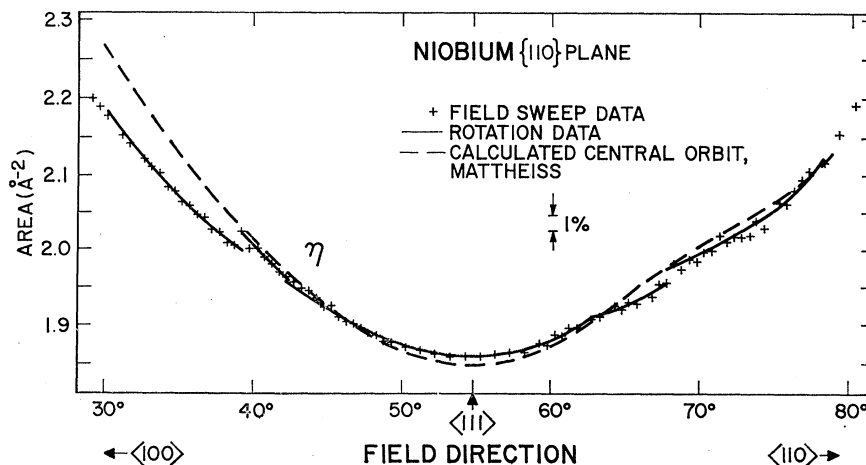
Nb with the exception of some of the details of the α , α' , and α'' branches. One discrepancy is the absence in the present data of an area near $[100]$ of 0.08 Å^2 .

B. Specific Aspects of Results

1. ν Branches

The ν orbits dominate the data at most orientations in both niobium and tantalum. The splitting of the branches ν_1 and ν_2 in both symmetry planes indicates that those parts of the Fermi surface on which these

FIG. 4. Extremal Fermi-surface areas in niobium as a function of angle in the $(1\bar{1}0)$ plane for the H intersection of the jungle gym. Discontinuities in rotation data are real and probably result from protrusions on the surface.



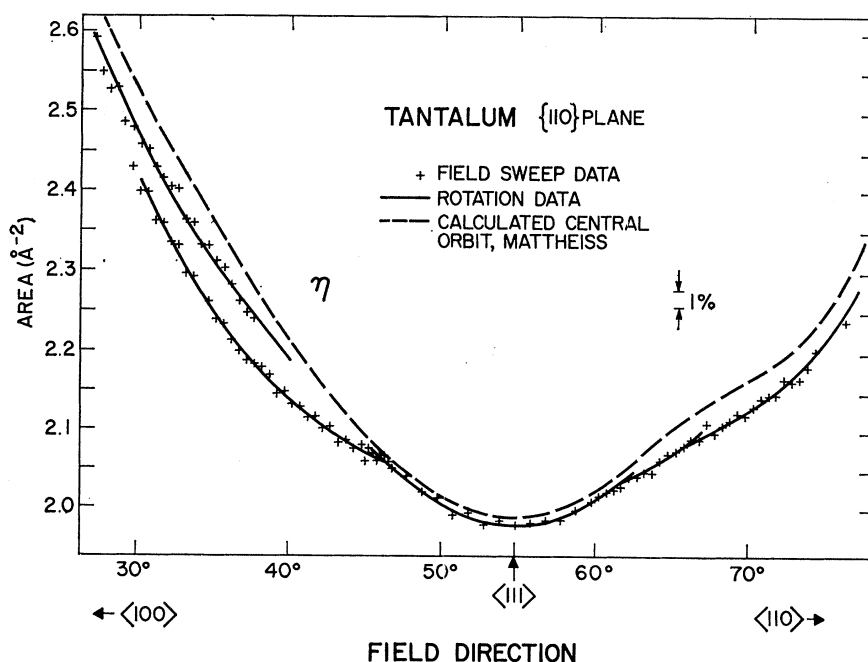


FIG. 5. Extremal Fermi-surface areas in tantalum as a function of angle in the $(1\bar{1}0)$ plane for the H intersection of the jungle gym. Discontinuities in rotation data are real and probably result from protrusions on the surface.

orbits lie are not figures of revolution; and the off-axis absolute minimum for ν_1 indicates that the actual shape is severely distorted from that of an ellipsoid, bulging out along the NT line. This is consistent with the calculated Fermi surface for both Ta and Nb. In fact, early band-structure calculations² indicated that there was the possibility that the distorted ellipsoids at N

might have necks along the NT line, thereby joining them with the jungle gym. If these necks existed, then the ν_2 orbits would not exist in the $(1\bar{1}0)$ plane and the $\nu_{5,6}$ orbits would not exist near the $[111]$ direction. The data in Fig. 2 and 3 clearly indicate the existence of ν_2 and thereby absence of NT necks.

2. α Branches

The arms on the third-zone jungle-gym hole surface of the APW Fermi surface support minimum area orbits, α orbits, for fields near $\langle 100 \rangle$ directions. In both Ta and Nb, sets of frequencies were observed near $\langle 100 \rangle$ axes, with frequency variation more rapid than that of a cylindrical surface, consistent with the hyperboloidal type surface of the model. In Nb these arm cross sections are about one-fourth the ellipsoid cross sections, whereas in Ta they are about two-thirds the ellipsoids. Assuming the arm orbits to be circular, the $\langle 100 \rangle$ areas of 0.138 and 0.263 \AA^{-2} yield diameters of 0.22 (ΓH) and 0.30 (ΓH) for Nb and Ta, respectively. These diameters are in excellent agreement with galvanomagnetic results.⁷

In Ta the exact range of the α oscillations is somewhat uncertain because of the complexity of the data, but they were observed at least 25° from the $\langle 100 \rangle$ axes. In Nb the angular range of the α branch seems to be 35° in the $(1\bar{1}0)$ plane and 30° in the (001) plane, and an anomalous amplitude dependence as a function of angle was observed. Other frequencies of approximately the same magnitude were observed over narrow ranges, and are labeled α' and α'' in Fig. 2. Still another frequency was observed within 20° of $[100]$ but is not shown in Fig. 2 because it was not possible to determine whether it was 21% larger or 21% smaller than the α frequency.

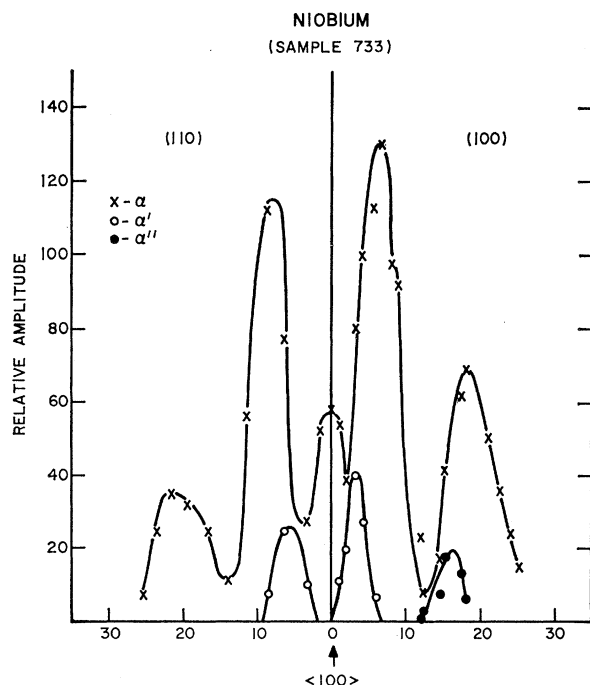


FIG. 6. Amplitude variation of dT/dH with angle in the $(1\bar{1}0)$ and (001) planes for α , α' , α'' frequencies. The lines connecting the points serve only to distinguish the α , α' , and α'' data.

The α'' branch was also studied in the plane that passes through the $[010]$ axis and 15° from the $[100]$ axis, and was found to extend 3° from the (010) plane. An additional feature of the data is that the amplitude of both the α' and α'' frequencies exhibits a strong correlation with the unusual amplitude variation of the α frequencies as shown in Fig. 6. That is, the α' and α'' amplitudes were large near regions for which the amplitude of the α frequencies was at a minimum.

Two possible explanations of both the α' and α'' branches exist that are consistent with the APW Fermi surface. One assumes noncentral orbits on one or the other of the second- and third-zone hole surfaces and the other involves magnetic breakdown between these surfaces. The second-zone hole surface shown in Fig. 2(a) lies just within the third-zone jungle-gym intersection at Γ . In the absence of spin-orbit interactions there are points of accidental degeneracy between the two surfaces in the $\{110\}$ and $\{100\}$ planes (see Fig. 4 of Ref. 4). This degeneracy is lifted by spin-orbit effects so there is no actual contact, but the surfaces remain distorted near those points. Since the APW closed second-zone hole surface bulges appreciably along the $\langle 100 \rangle$ axes, especially in Nb, these distortions could be sufficient to provide extremal orbits for fields near $\langle 100 \rangle$ axes. If so, the question arises as to why only one additional frequency is observed, since the occurrence of a relative maximum due to such a distortion normally would necessitate the simultaneous occurrence of a relative minimum, and conversely. However, the amplitudes could be quite different and/or the two orbits could be nearly identical in frequency and therefore difficult to resolve. Similar possibilities arise for extremal orbits on the jungle gym near $\langle 100 \rangle$ directions due to the corresponding distortions, and the same arguments apply. The amplitude dependence of other α frequencies is not understood.

Another possibility for the existence of the α' and α'' branches is offered by magnetic breakdown between the second- and third-zone surfaces at those points where the absence of spin-orbit effects would allow the accidental degeneracies. The region where α'' frequencies are observed just corresponds to a region where three breakdown points are coplanar, and the correlation of amplitudes of the α , α' , and α'' frequencies is suggestive of breakdown.

We conclude that either explanation or a combination of both can account for the experimental data for Nb. In Ta the larger spin-orbit splitting could eliminate the possibility of magnetic breakdown and/or smooth out the distortions of the Fermi surface so that the subsidiary extrema would not exist.

3. η Branches

With fields near 100 kOe, a set of faster frequencies were observed in the $(1\bar{1}0)$ plane with a minimum occurring at the $[111]$ axis, as shown in Figs. 4 and 5 for Nb and Ta, respectively.

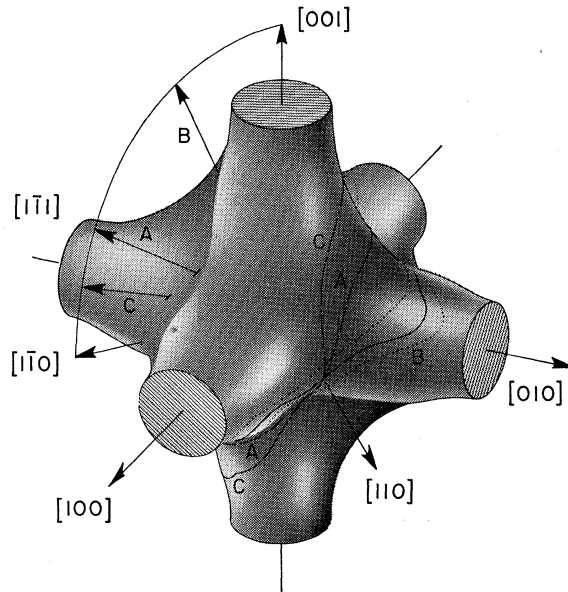


FIG. 7. Three-dimensional sketch of the H intersection of the jungle-gym surface with an indication of some of the orbits which may be the source of multiplicities shown in Figs. 4 and 5.

Both the γ_2 orbits about the Γ -centered intersection of the jungle gym, and the η orbits about the H -centered intersection show the required minimum area in the $[111]$ direction, but the quantitative agreement between the APW Fermi surface and the experimental data is $\sim 1\%$ if we assign these higher frequencies to the η orbits. The discrepancy would be 35% for Ta and 75% for Nb of the experimental frequency if the γ_2 orbit is assumed. Also the calculated masses of the γ_2 orbit are so high that their observation is not expected.

The results shown in Figs. 4 and 5 exhibit a multiplicity of frequencies over certain ranges for this branch in both Nb and Ta. These are compatible with the APW calculations, which has lumps on the jungle-gym surface such as to allow noncentral extremal orbits. The three-dimensional sketch of the H intersection in Fig. 7 illustrates the point by showing the calculated protrusions along the $\langle 100 \rangle$ directed arms and some typical orbits. In particular, for fields near $\langle 111 \rangle$ central orbits such as A in Fig. 7 exist. As the field is tilted toward $\langle 100 \rangle$ in a $\{110\}$ plane, at some angle the central orbit must traverse the tops of four of these protrusions, such as B in Fig. 7, and it is quite probable that for some angular range the central orbit will be due to a relatively maximum area, and smaller non-central minimum areas will also exist. The latter are indicated in Fig. 7 by the two equivalent dotted line orbits on either side of the B orbit. A similar situation occurs when the field is rotated toward a $\langle 110 \rangle$ direction in a $\{110\}$ plane, for which the central orbit is indicated by the C orbit in Fig. 7. In this case, the central orbit traverses only two protrusions. The non-central orbits are not shown but again are expected to be relatively minimum areas.

TABLE I. Effective mass summary.

Orientation	Surface	Niobium ($1+\lambda=1.82$)				
		Area (exp) (\AA^{-2})	Area (APW) (\AA^{-2})	$m^*_{\text{(exp)}}$	$m^*_{\text{(APW)}}$	$m^*/m^*_{\text{(APW)}}$
[100]	Ellipsoid	0.815	0.855	1.60	0.97	1.65
[100]	Jungle gym	0.138	0.117	1.12	0.57	1.97
[111]	Ellipsoid	0.647	0.663	1.28	0.73	1.75
[110]	Ellipsoid	0.657	0.677	1.22	0.70	1.74
Tantalum ($1+\lambda=1.65$)						
[100]	Ellipsoid	0.436	0.395	1.09	0.60	1.82
[100]	Jungle gym	0.279	0.292	1.35	0.84	1.61
[111]	Ellipsoid	0.472	0.448	1.06	0.60	1.77
[110]	Ellipsoid	0.472	0.442	1.18	0.61	1.94
[110]	Ellipsoid	0.580	0.562	1.35	0.75	1.80

The data shown in Figs. 4 and 5 do not exhibit all the features required to be completely consistent with the above interpretation. In particular, in some regions the central orbit is not observed, e.g., in Nb, Fig. 4, for θ less than 39° and between 65° and 68° , and in Ta, Fig. 5, for θ between 40° and 45° and again between 63° and 66° . Similarly, noncentral orbit frequencies are missing in Nb, Fig. 4, between 39° and 42° . These negative results can be attributed to any of a variety of reasons which are considerations of relative amplitudes and are not considered significant. A puzzling feature about this interpretation of the data is the way which the noncentral orbit near $\theta=66^\circ$ in Ta (Fig. 5) appears to merge with the supposedly central orbit observable at larger angles, since the noncentral should always be smaller than the central one. This point has not yet been reconciled, but because of the complexity of the calculated surface, it is not considered of great import, and the conclusion remains that all the η frequencies arise from orbits about the H intersection of the jungle-gym surface.

4. γ_1 , γ_2 , and Δ Branches

The APW surface supports a number of other orbits, namely hole orbits (γ_1) about the second-zone closed hole surface at Γ , hole orbits (γ_2) about the Γ -centered intersection of the third-zone jungle-gym surface, and electron orbits (Δ) within the square ring formed by four connecting jungle-gym arms. None of these have been observed, and all are estimated⁴ to have higher masses than the orbits which have been observed.

C. Cyclotron Mass Results—Mass Enhancement

Cyclotron masses have been determined from the temperature dependence of the oscillation amplitudes at a number of orientations for Nb and Ta. The results from the MTO experiments are summarized in Table I which also includes the masses obtained in the APW

calculation. It is clear from the table that the experimental masses are substantially larger than the calculated masses. This “mass enhancement” can be due to a number of influences—e.g., electron-phonon interaction, electron-electron interaction, paramagnon effects, and perhaps others. The first of these, phonon enhancement, is likely to be the most important and has been calculated by McMillan⁵ for a variety of materials. McMillan’s results for the phonon enhancement are expressed in terms of a constant λ such that

$$m^*_{\text{exp}} = (1+\lambda)m^*_{\text{calc}}.$$

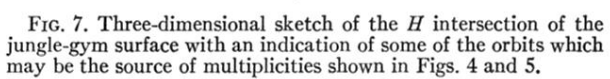
Therefore, in the table we have listed the ratio of ($m^*_{\text{exp}}/m^*_{\text{calc}}$) for comparison with $(1+\lambda)$. In Nb the measured enhancements are about 7% less than McMillan’s value of 1.82, and in Ta the measured values are about 10% higher than the calculated value of 1.65. The masses as determined from the torsion balance studies of Ta at 30 kOe are $\sim 10\%$ higher than the values in the table. In view of the uncertainty of the cyclotron mass measurements no statement can be made about possible anisotropy of the mass-enhancement factor.

V. SUMMARY

Several sections of the Fermi surfaces of Nb and Ta have been determined, and appear to be qualitatively almost identical for the two materials. Comparison with the APW Fermi surface obtained by Mattheiss gives good agreement with the present data. The sections observed are identified as a set of six third-zone closed hole surfaces (warped ellipsoids) centered at N in the bcc Brillouin zone, and a multiply connected third-zone hole surface (jungle gym) with arms along $\langle 100 \rangle$ directions intersecting at Γ and H . The second-zone closed hole surface centered at Γ , predicted by the APW model, and several possible orbits on the jungle-gym surface have not been observed, probably because of their expected higher effective masses. Measured effective masses are consistently larger than the calculated masses, and the enhancement is found to be in reasonable agreement with the values derived from the superconducting transition temperatures.

ACKNOWLEDGMENTS

We thank R. R. Soden for supplying the single crystals of Nb and Ta. We are indebted to L. F. Mattheiss for many helpful discussions concerning the band structure of these materials and for the communication of the results of his calculations prior to publication. We also wish to thank W. A. Reed for helpful discussions concerning the galvanomagnetic effects and R. J. Schutz for technical assistance.



may be the source of multiplicities shown in Figs. 4 and 5.